Vol 17 No 8, August 2008
1674-1056/2008/17(08)/3040-14

Chinese Physics B

© 2008 Chin. Phys. Soc.
and IOP Publishing Ltd

Electronic structure and physical properties of ScN in pressure: density-functional theory calculations*

Guan Peng-Fei(管鹏飞)[a)†], Wang Chong-Yu(王崇愚)[b)], and Yu Tao(于 涛)[c)]

[a)] *Central Iron and Steel Research Institute, Beijing* 100081, *China*
[b)] *China Centre of Advanced Science and Technology (World Laboratory), Beijing* 100190, *China*
[c)] *Department of Physics, Tsinghua University, Beijing* 100084, *China*

(Received 12 May 2008; revised manuscript received 26 May 2008)

Local density functional is investigated by using the full-potential linearized augmented plane wave (FP-LAPW) method for ScN in the hexagonal structure and the rocksalt structure and for hexagonal structures linking a layered hexagonal phase with wurtzite structure along a homogeneous strain transition path. It is found that the wurtzite ScN is unstable and the layered hexagonal phase, labelled as h_o, in which atoms are approximately fivefold coordinated, is metastable, and the rocksalt ScN is stable. The electronic structure, the physical properties of the intermediate structures and the energy band structure along the transition are presented. It is found that the band gaps change from 4.0 to 1.0 eV continuously when c/a value varies from 1.68 to 1.26. It is noticeable that the study of ScN provides an opportunity to apply this kind of material (in wurtzite[h]-derived phase).

Keywords: full-potential linearized augmented plane wave (FLAPW), band gap, phase transition
PACC: 7125

1. Introduction

Transition metal nitrides have a wide range of technological applications, due to their excellent physical properties that include high hardness, mechanical strength, and high melting point. These materials crystallize in the rocksalt structure and can be either metallic or semiconducting. Furthermore, there has also been a long interest in another transition metal nitride: namely ScN. Recently, achieved was the smooth epitaxial growth of singly oriented ScN films,[1−3] showing the possibility of using ScN as an electronic material. ScN is believed to be a narrow-gap semiconductor and its lattice constant is very similar to that of GaN (a wide-gap semiconductor), then combining the two kinds of semi-conductors into the form of heterostructure could be of great interest in the fabrication of electronic devices. The first-principles calculations by using some techniques, such as screened-exchange (SX) and quasi-particle corrections,[4,5] have shown that ScN is a semiconductor. The calculations[4] have also shown that ScN, YN, GdN, and LaN are indirect semiconductors with gaps of about 1–2 eV, and ScN has a very small lattice mismatch with GaN($< 2\%$), which perhaps can be useful for combining ScN with GaN into a GaN/ScN hetero-structure or ScGaN alloy. A similar situation also occurs in YN and InN. Most of the previous studies on ScN mainly focused on the ground-state structure (the rocksalt phase), while Farrer and Bellaiche[6] reported on the discovery of another metastable phase in ScN, i.e. a layered hexagonal (nonpolar) phase that is five-times coordinated (denoted as h_c-ScN, a phase similar to that found in MgO,[7]) which has a total energy that is about 316 meV/(2 atoms)[6] higher than the value calculated from the ground-state rocksalt phase of ScN.[8−10] Ranjan *et al*[11] have predicted that applying a compression in-plane strain to h_c-ScN can result in a very high piezoelectric response, as well as the tuning of the electronic band gap in a large visible range. In other words, it can be a multifunctional material. The super-lattices were studied,[12,13] which are composed of alternating n layers of ScN with n layers of GaN (or InN). It is found that the super-lattices undergo an isostructural phase transition (from a wurtzite-derived phase to an h-derived phase) in the presence of a hydrostatic pressure, and such a phase transition is also accompanied by the changes of the optical and dynamical properties. Some of these properties are technologi-

*Project supported by the State Key Development Program for Basic Research of China (Grant No 2006CB605102).
†E-mail: miracle.fei@gmail.com

cally promising, e.g. when the increase of the portion of the nontransition-metal cations, the band gap of the super-lattices is predicted to range from near infrared to green for wurtzite-derived InN/ScN superlattices and from near infrared to blue/ultraviolet for GaN/ScN systems in their wurtzite-derived phase. Little and Kordesch,[14] grew ScGaN by using the sputtering technique and reported on amorphous or microcrystalline films and a linearly decreasing optical band gap (from 3.5 down to 2.0 eV) with Sc concentration increasing.[14] Recently, using the molecular beam epitaxy technique, Costel *et al*[15] reported on the growth evidence for the meta-stable layered hexagonal phase. Also, they have suggested that for $Sc_xGa_{1-x}N$, at a regime $x < 0.17$ it has a wurtzite-like structure but with local lattice distortions and an anisotropic lattice expansion occurs with x increasing, where a increases much more than c, and so the value of c/a decreases.

In this paper, we present our results on the transition path linking wurtzite with h_o in ScN which is important for forming wurtzite-derived (or h-derived) phase with other compounds (such as GaN) and for investigating the phase stability of ScN. It is found that for ScN, wurtzite phase is unstable towards an intermediate structure between wurtzite and rocksalt, which is hexagonal structure, called h_o structure, and will be described in detail below. We here present energy band structures and charge densities to show the formation of the new bonds as we move from wurtzite structure to h_o structure. The optical properties accompanied by the transformation of phase are also given in the paper.

The rest of the paper is organized as follows. First we discuss the geometric aspects in Section 2. In Section 3, we provide the necessary information on our computational method. Next, the result for ScN is clearly discussed in Section 4. In this section, the lattice character, the total energy and band structure results for rocksalt (RS), hexagonal (h_o) structure, and wurtzite (WZ) structure are all presented. We also give the results on the band structure of the intermediate structures along the transition for ScN, and the information about the different charge densities of the intermediate structures which allows us to monitor the bond formation during the transition. In summary, we mainly focus on the difference charge densities and the bond formation along the transition, and on the recent information about the band structure along the transition path.

2. Crystal structures

Here, we investigate a particular kind of hexagonal crystal structure that is characterized by three parameters, i.e. the lattice constant a, the c/a ratio, and the internal parameter u that determines the relative position of the two ideal hexagonal closed-packed sublattices. The primitive lattice vectors of this structure are[6]

$$\boldsymbol{a}_1 = a\left(\frac{1}{2}\boldsymbol{x} - \frac{\sqrt{3}}{2}\boldsymbol{y}\right), \tag{1}$$

$$\boldsymbol{a}_2 = a\left(\frac{1}{2}\boldsymbol{x} + \frac{\sqrt{3}}{2}\boldsymbol{y}\right), \tag{2}$$

$$\boldsymbol{a}_3 = c\boldsymbol{z}, \tag{3}$$

where a and c are the two different lattice parameters, c/a is the axial ratio, and $\boldsymbol{x}$, $\boldsymbol{y}$, $\boldsymbol{z}$ are the unit vectors along the Cartesian axes. The primitive unit cell contains four atoms: two atoms of type A (e.g. N) located at $\boldsymbol{r}_1$ and $\boldsymbol{r}_2$ separately, and two atoms of type B (e.g. Sc) located separately at $\boldsymbol{r}_3$ and $\boldsymbol{r}_4$, where

$$\boldsymbol{r}_1 = \frac{1}{3}\boldsymbol{a}_1 + \frac{2}{3}\boldsymbol{a}_2, \tag{4}$$

$$\boldsymbol{r}_2 = \frac{2}{3}\boldsymbol{a}_1 + \frac{1}{3}\boldsymbol{a}_2 + \frac{1}{2}\boldsymbol{a}_3, \tag{5}$$

$$\boldsymbol{r}_3 = \frac{1}{3}\boldsymbol{a}_1 + \frac{2}{3}\boldsymbol{a}_2 + u\boldsymbol{a}_3, \tag{6}$$

$$\boldsymbol{r}_4 = \frac{2}{3}\boldsymbol{a}_1 + \frac{1}{3}\boldsymbol{a}_2 + \left(\frac{1}{2} + u\right)\boldsymbol{a}_3, \tag{7}$$

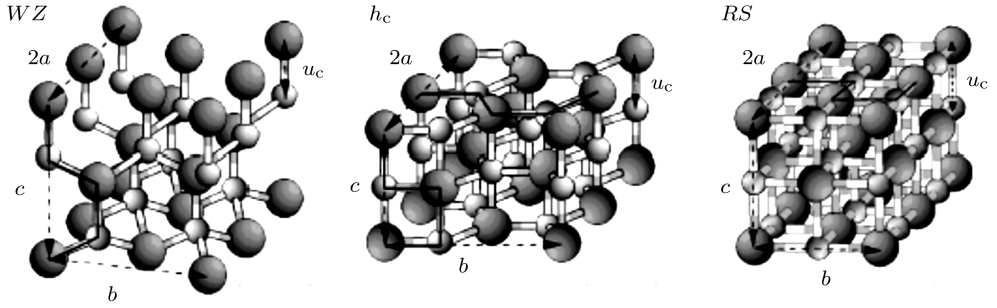
where u is the dimensionless internal parameter. As is known, in the ideal wurtzite structure (see Fig.1(a)) with space group P63mc, characterized by equal bond lengths, c/a is $\sqrt{8}/3$ and u is 3/8, and in the hexagonal structure (see Fig.1(b)) with space group P63/mmc, which has been found in MgO and is nearly five-times coordinated.[7] u is 1/2. The parameters u and c/a, however, are not independent of each other, because for any given value of c/a specifying a uni-axial strain, u must be determined such that there is no force on the atoms. We can find that near the ideal wurtzite structure, u increases linearly with the decrease of c/a but eventually it starts varying faster and then locks into a value of 1/2, and the two bond lengths perpendicular to the mirror plane are almost equal to the three bond lengths in the plane. Then the space group changes from $P6_3mc$ to $P6_3/mmc$ due to the introduction of an extra mirror plane. It is different from the layered material h-BN, as is well known, h-BN structure is essentially three-fold coordinated because the

interlayer distance is too large to form a bond. Under the compression of this structure along c/a, it has been found[8] to be converted into a wurtzite structure at some critical value of c/a that is reduced by forming a bond perpendicular to the plane. This breaks the mirror plane symmetry and the bonding becomes tetrahedral. It can also be found in ScN. So we can indicate that the wurtzite structure with $P6_3mc$ degenerates into a more symmetric $P6_3/mmc$ group either by forming a perpendicular bond or by destroying the perpendicular bond.

Table 1. Crystal parameters in wurtzite, h_o, and rocksalt structures.

crystal parameters	ideal WZ	h_o	RS
c/a	1.633	about 1.2[a)]	1.0
u	3/8	1/2	1/2
b/a	$\sqrt{3}$	$\sqrt{3}$	1.0
v	1/3	1/3	1/2
point group	Fm3m	$P6_3mmc$	$P6_3/mc$
polarity	nonpolar	nonpolar	Polar

[a)]It is determined by total energy minimizations, described later in paper.



(a) (b) (c)

Fig.1. The structure of ScN, where panel (a) is for wurtzite structure, panel (b) for h_o structure, and panel (c) for rocksalt structure.

The values of the parameters c/a, u, b/a, and v in WZ, h_o and RS structures are indicated in Table 1. Except for the value of c/a in h_o structure, which is determined by minimizing the total energy, the other parameters are completely determined by geometry. The general problem can then be stated as mapping out the energy landscape in the parameter space of external strain, c/a and b/a specifying the orthorhombic strain. In principle, we have to find the 'best' u and v to minimize the internal strain energy and the equilibrium volume V. Then we can identify the number of local minima and the lowest-energy paths as well as the minimum barrier to move from one local minimum to another in this energy landscape. In practice, we take a single cut to avoid exploring the whole landscape.

3. Calculation method

The calculations are performed in the framework of density functional theory.[16] We have employed the full potential linearized augmented plane wave (FP-LAPW[17]) method as implemented in the WIEN2K code.[18] The exchange and correlation effects are treated by using the generalized gradient approximation (GGA) given by Perdew, Burke, and Ernzerhof.[19] The technical details of our calculations are as follows. We treat the core states fully relativistically and the valence states scalar also relativistically, and we use angular momenta up to $l_{max} = 10$ in the muffin-tin spheres for both the wave functions and the charge density in the self-consistent cycles. And the cutoff energy for the plane-wave expansion in an interstitial region is 19.5 Ry.

Also, we relax the positions of all the atoms until the forces are less than 1mRy/a.u. The muffin-tin radii are $R_N = 1.8$ and $R_{Sc} = 2.0$ bohrs for N and Sc atoms, respectively. And 84, 80 and 76 k points in the irreducible part of the Brillouin zone (IBZ) are for the rocksalt structure, the hexagonal (h_o) structure and the wurtzite structure, respectively. With respect to the N_2 molecule, the bond length is calculated to be 0.11 nm within the GGA, which is in good agreement with other calculations.[4] The experimental value is 0.1098 nm.[20]

4. Results and discussion

4.1. Electronic structure and physical properties of the special structures

4.1.1. Lattice parameters and total energy properties

The lattice constants, bulk moduli, and total energy are obtained by using the GGA and listed in Table 2. Where possible, we have included the results of other *ab initio* calculations and measurements. For *RS*-ScN, only volume is allowed to relax, for all other crystal parameters are fixed due to the crystal symmetry. For h_o-ScN, b/a and v are fixed and c/a, u and volume are allowed to relax. For WZ-ScN, we relaxed u and volume; other structural parameters are fixed due to the crystal symmetry.

Table 2. Comparison between the local-density-approximation(LDA)-predicted properties of the *RS*-, h_o-, WZ-ScN. a, c/a, u, V and B_0 are the in-plane lattice constant, axial ratio, internal parameter, volume of the primitive cell, and bulk modulus, respectively. d_{nn} denotes the distance between the nearest neighbours. ΔE is the difference in total energy between the considered phase and the rocksalt structure, and the 2 atoms include one Sc atom and one N atom of the primitive unit cell.

property		*RS*-ScN	h_o-ScN	WZ-ScN
a/nm		0.452	0.373	0.345
		0.454[a)]	0.366[b)]	0.349[a)]
	Expt.	0.450[c)], 0.444[d)]	-	-
c/a		1	1.208	1.633
		-	1.207[b)]	1.60[a)]
u		1/2	1/2	0.3815
		-	-	0.38[a)]
V/nm^3		0.04614[0.0480]	0.05434[0.0514]	0.05838[0.05434]
		0.04680[a)]	0.05125[b)]	0.05882[a)]
B_o/GPa		195	164	140
		201[a)]	181[b)]	-
d_{nn}/nm		0.226	0.215–0.225	0.200–0.210
ΔE/(eV/2 atoms)		0	+0.184	+0.449

[a)] Reference [10]
[b)] Reference [6]
[c)] References [21-24]
[d)] Reference [25]

It has been found that rocksalt has a ground-state structure of ScN, with $a = 0.452\,\text{nm}$, $B_0 = 195\,\text{GPa}$, and cohesive energy $E_0 \approx 1.00\,\text{Ry}$. Experimental values are $a = 0.4501\,\text{nm}$ and $B_0 = 182 \pm 40\,\text{GPa}$ for the lattice constant and bulk modulus, respectively.[2] The agreement between the theory and experiment is very good. There is an additional local minimum in the h_o structure with $a = 0.373\,\text{nm}$, $c/a = 1.208$ and total energy that is $0.184\,\text{eV}/(2\text{ atoms})$ higher than the calculation, which is in good agreement with earlier calculations.[6] We also give the results of the wurtzite structure with $c/a = 1.633$, $a = 0.345\,\text{nm}$, $u = 0.3815$ and total energy that is $0.449\,\text{eV}/(2\text{ atoms})$ higher than the calculation. Also, we note that the lattice constant a and the length of bonds both increase, while the equilibrium volume decreases as we move from wurtzite to h_o to rocksalt structures due to the increase of coordination number. From this decreasing volume we note that there is a decrease in total energy; in other words, the cohesive energy of the solid becomes higher. Progressively, the bulk moduli increase as expected.

Finally, we have also obtained the curve for energy versus volume for each structure and derived from them the bulk modulus in each structure, and the transition pressures between the different structures using the common tangent construction. The curves for total energy as a function of volume are shown in Fig.2, where it is indicated that the lowest-energy structure is correctly found to be of rocksalt and that in order to convert it into h_o-ScN we need a negative pressure. At this pressure, the volume is expanded to reach the value $V_1/V_{RS} = 1.04$ and then the volume would be discontinuously expanded, arriving at the value $V_2/V_{RS} = 1.24$ and entering into the h_o-ScN phase, where V_{RSi} is the volume of *RS*-ScN at zero

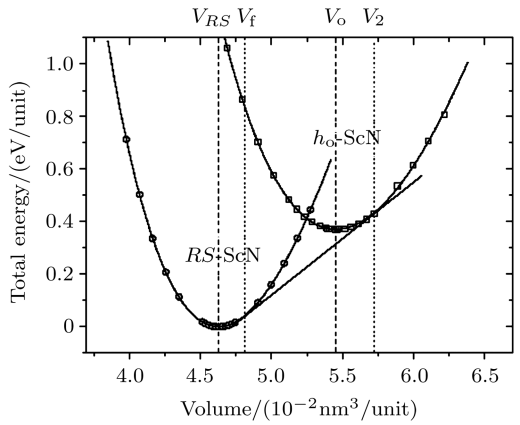


Fig.2. The curves for total energy as a function of volume for RS- and h_o-ScN and the common tangent construction, where V_{RS} and V_o are the equilibrium volumes of RS-ScN and h_o-ScN at zero pressure, respectively. V_1 and V_2 are the volumes of RS-ScN and h_o-ScN at the phase-transition pressure, respectively.

pressure. This is of course somewhat unphysical because one cannot apply a negative pressure in the laboratory. However, one may think of alloying with another compounds (such as YN) to expand the lattice constant, and in this sense the result shows how big an expansion should be needed before the equilibrium between the meta-stable h_o-ScN phase and the stable rocksalt phase occurs. Of course, alloying with other elements will have other effects besides the expansion, so this consideration is applicable only for a limited number of cases in reality.

4.1.2. Electronic structure and optical properties

The energy band structures are also obtained and presented in Figs.3(a), 3(b) and 3(c) for RS-, h_o-, and WZ-ScN structures, respectively. The solid lines correspond to the bands at the equilibrium volume of each phase.

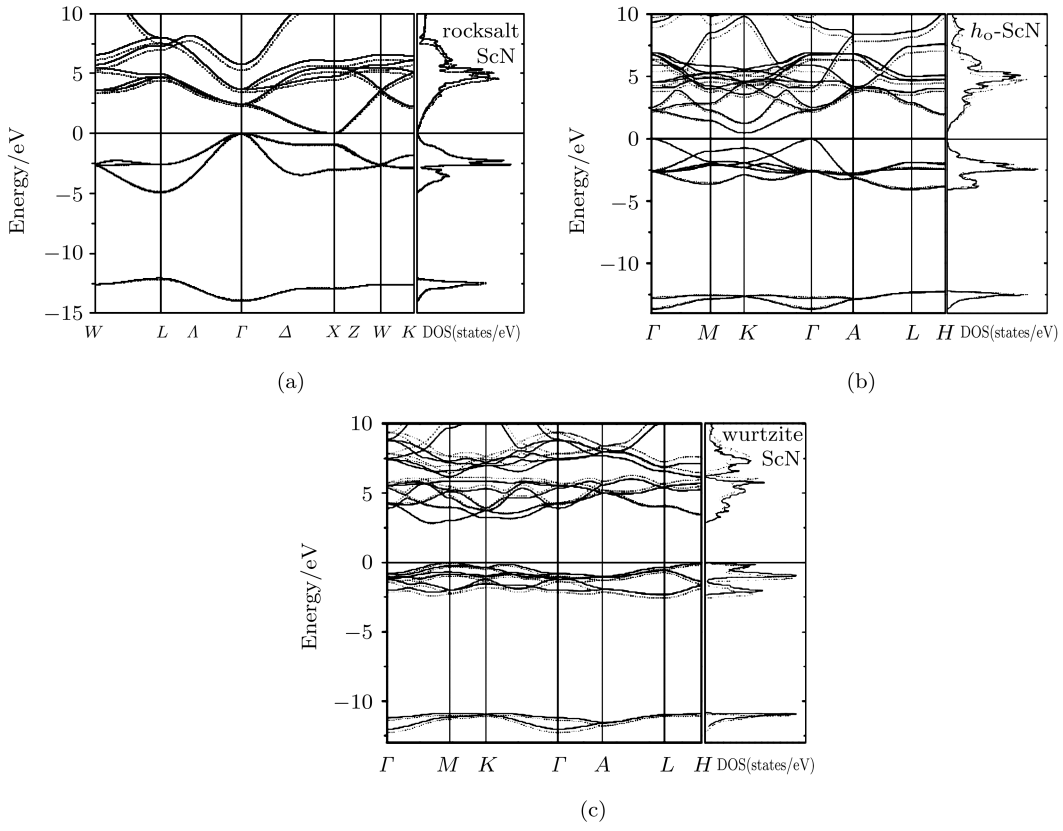


Fig.3. Band structures of ScN, where panel (a) shows the Band structures of RS-ScN, with solid lines bing for equilibrium volume V_{RS} and dashed lines for expanded volume V_1, corresponding to the common tangent point shown in Fig.2; panel (b) displays the Band structures of h_o-ScN, with solid lines being for equilibrium volume V_o and dashed lines for expanded volume V_2, corresponding to the common tangent point shown in Fig.2; panel (c) describe the Band structures of WZ-ScN, with the solid lines being for equilibrium volume VWZ and dashed lines for the equilibrium volume V_o of h_o-ScN.

In the terms of electronic structure, we may note that this is accompanied by an increase in valence bandwidth and a downward shift of the centre of gravity of the N 2s valence band. This means that some of the occupied states obtain lower energies (with respect to the valence-band maximum (VBM) and this is consistent with the band structure making a less contribution to the total energy. This also accords with the formation of additional bonds which will be described more clearly later.

Table 3. Characteristic energy gaps of the band structures shown in Figs.3(a)–3(c), where $E_{\rm Ns} - E_{\rm Np}$ is the energy gap between the Ns band and the valence band complex, $E_{\rm p} - E_{\rm s}$ is the $\rm N_p - N_s$ energy gap at Γ, $Eg(\Gamma)$ is the zone-centre metal d band splitting at Γ and W is the upper valence-band width. The values in square brackets are the parameters at the volume corresponding to the common tangent construction shown in Fig.2.

energy gaps		RS-ScN	$h_{\rm o}$-ScN	WZ-ScN
nature of the band gap		indirect	indirect	indirect
		$\Gamma \to X$	$\Gamma \to K$	$M \to \Sigma$
$E_{\rm g}$/eV		~ 0[0.05]	0.47[0.53]	2.84[2.87]
		0[a], 1.58[b]	0.25[c]	3.0[a]
	Experimental	1.3 ± 0.3[d]	-	-
$E_{\rm g}(\Gamma)$/eV		2.43[2.29]	2.30[2.23]	4.72[5.14]
W/eV		4.95[4.81]	4.06[3.90]	2.30[2.50]
$E_{\rm Ns} - E_{\rm Np}$/eV		7.15[7.30]	8.20[8.30]	8.62[8.46]
$E_{\rm p} - E_{\rm s}$/eV		14.01[13.86]	-	-

[a] Reference [9]
[b] Reference [4]
[c] Reference [6]
[d] Reference [7]

Our calculated RS-ScN LDA band gap is almost zero and indirectly located from Γ to X, which is in good agreement with other LDA calculations.[4,10] It is well known that the energy band gaps are not given accurately by the Kohn-Sham eigenvalues in LDA because they do not truly represent quasi-particle excitation energies.[26–29] However, the corrected LDA gaps are only weakly dependent on the structure. If we compare our RS-ScN LDA band gap with a measured band gap of 1.3 eV, we can estimate that a correction of 1.3 eV is applicable for the other structures. Considering this correction, the predicted band gaps of WZ- and $h_{\rm o}$-ScN will be 4.13 eV and 1.77 eV, respectively. Note that it will probably be underestimated slightly, for when the gap increases, the self-energy correction also increases because the gap correction is inversely proportional to the band gap. In $h_{\rm o}$-ScN the VBM is located at Γ, while the conduction- band minimum (CBM) is at K. This accords with the earlier work by Farrer and Bellaiche[6] They found the value of the LDA band gap to be 0.25 eV. In WZ-ScN the CBM is located away from Γ (approximately 70% away from $\Gamma \to M$), while the VBM is at M. This is consistent with the earlier work[5,11] as far as the location of the band extremum is concerned and close to the value of the LDA gap, which was obtained to be about 3 eV.[5]

We can find that the shape of 2s band almost does not change from wurtzite phase to $h_{\rm o}$ phase, but the shape of top valence-band changes significantly. The LDA band gaps are listed in Table 3. $E_{\rm Ns} - E_{\rm Np}$ is the energy gap between the N s band and the valence band complex, $E_{\rm p} - E_{\rm s}$ is the $\rm N_p - N_s$ energy gap at Γ, $E_{\rm g}(\Gamma)$ is the zone-centre metal d band splitting at Γ and W is the upper valence-band width. It is found that when the volume is compressed from WZ to RZ, the upper valence band width will increase, but the band gaps will become smaller.

We have also examined the band structures of both RS- and $h_{\rm o}$-ScN at the transition pressure (compressed volume) and WZ-ScN at the volume $V_{\rm o}$ (the equilibrium volume of $h_{\rm o}$-ScN). These band structures are presented as dashed lines in Figs.3(a)–3(c). The band structures of RS and $h_{\rm o}$ structures deform in a similar way, with volume being compressed; the band gaps become smaller; the upper valence band widths increase. It suggests that the hydrostatic deformation potential is positive in RS-ScN and $h_{\rm o}$-ScN. The detailed variations in band gaps and band widths are summarized in Table 3.

The total partial densities of states (DOSs) for ScN studied are shown in Figs.4(a)–4(c) for the Sc atom and for the nitrogen atom of the bulk compound,

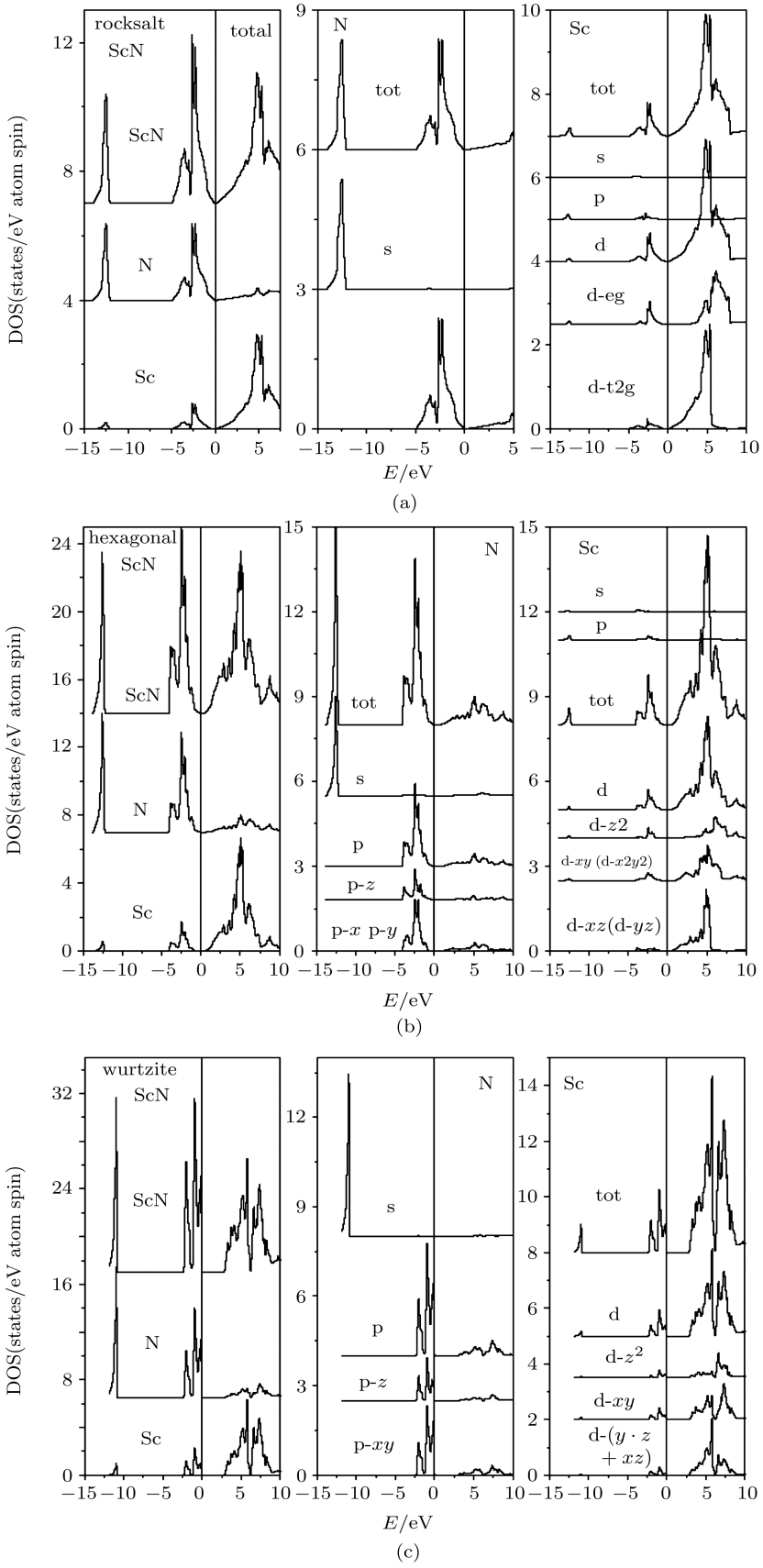


Fig.4. Partial densities of states and their state resolved components of ScN, where panel (a) is for *RS*-ScN, panel (b) for h_o-ScN, and panel (c) for *WZ*-ScN.

in additions to their states (s, p[p_i], d [d_i]) resolved DOSs. The quantities indicate that there is a strong hybridization between the N states and the Sc states with the energy position. The feature in the lowest energy case is that the N 2s derived state and the N state mixes with the s states of Sc atom in a conduction-band region. With respect to the valence-band complex, these are two high density regions separated by a low electron density region. At the bottom of the lower region involved are the bonding contributions of Sc s- Np states and above this involved are the bonding contributions of Sc d(and some p) - Np states. At the bottom of conduction-band, it is mainly due to Sc d states with some Np components. It is very interesting that the WZ-ScN bottom region of conduction-band is clearly split into two peaks due to a large difference in energy between σ^* and π^* bonds. These hybridizations are indicated from the decomposition of the partial DOSs into their s; p; and d contributions as shown in Fig.4(a)–4(c). Also, the upper valence-band width becomes smaller as the crystal is compressed from wurtzite structure to rocksalt structure.

4.2. Intermediate transition structures from WZ to h_o

4.2.1. Total energy and internal parameter

As mentioned in the previous sections, WZ-ScN is unstable, and the transition from WZ-ScN to RS-ScN can be studied in two parts: WZ-ScN-to-h_o-ScN and h_o-ScN-to-RS-ScN. As is known, no reason why we should first reduce c/a and then b/a in transforming from WZ to RS. Instead we need to explore the complete parameter space, which we will report later. Then we consider a transformation path where b/a is constant (equal to $\sqrt{3}$) and c/a is varying between their final values of ideal WZ and ideal h_o. This intermediate transition structure is important for forming wurtzite-derived (or h-derived) phase with other compounds (such as GaN).

The transition from WZ-ScN to h_o-ScN does not have any energy barrier and is obtained simply by minimizing the total energy with respect to the structural parameters. The curves for total energy and u as a function of c/a in a range of 1.68-to-1.208] are shown in Fig.5. Note that along the path from WZ-ScN to h_o-ScN the values of both b/a and v are fixed at those of WZ-ScN due to symmetries. However, u and volume are relaxed to obtain the minimum energy in the following way. The relaxed u and total energy as a function of c/a are first determined with the volume fixed at that of ideal h_o-ScN. In order to obtain the effect of volume on the relation, we also investigate the relation at different values of lattice parameter a. When the value of a is less than that of a_o (the equilibrium lattice constant of h_o-ScN), the relation is almost independent of volume (see the left panel in Fig.7). The left panel in Fig.6 indicates the volume that minimizes the energy at c/a and the u that is relaxed for volume, while the right panel in Fig.6 shows the simultaneous evolution of u.

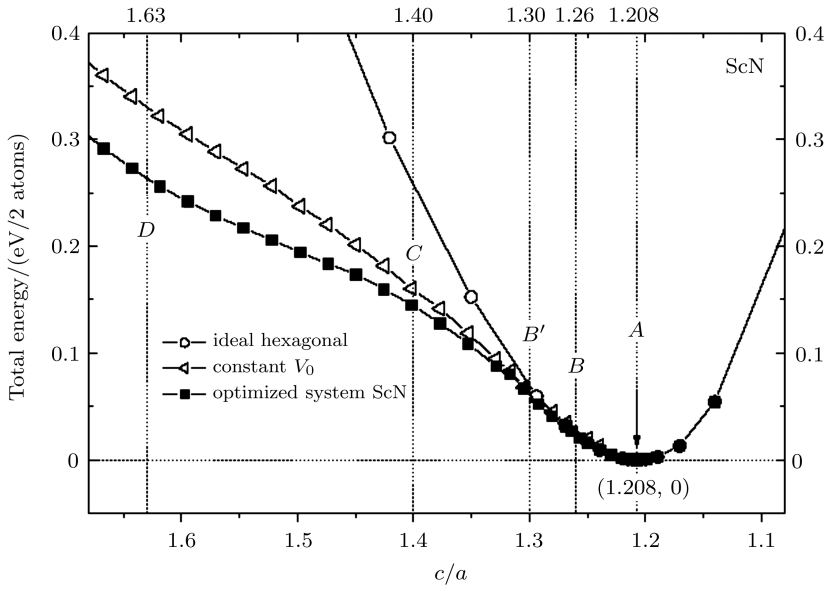


Fig.5. Curves for total energy per unit of ScN in the WZ-ScN → h_o-ScN transitions, where A, B, B', C and D are special points whose corresponding values of c/a are 1.208, 1.26, 1.30, 1.40 and 1.63, respectively.

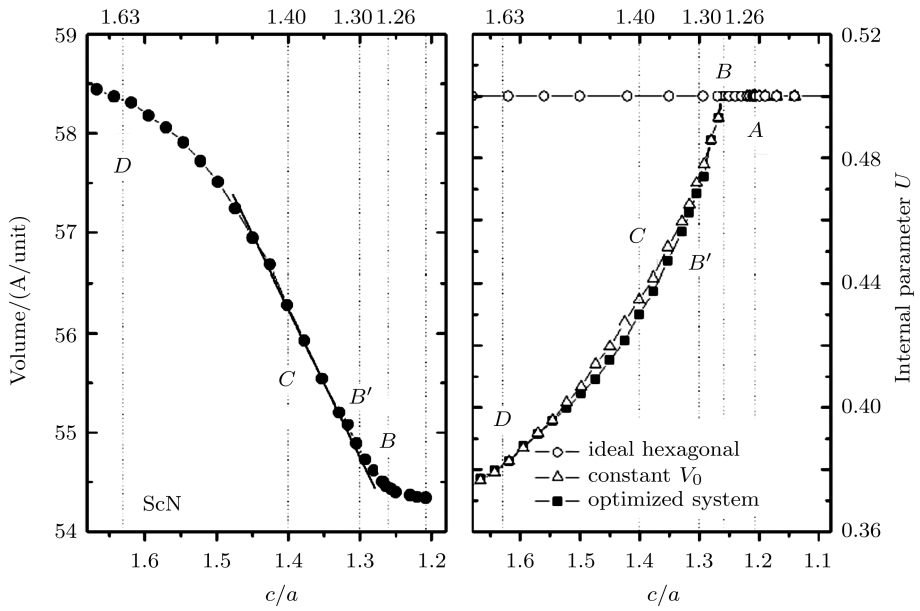


Fig.6. Curves for the energy minimizing volume and u used in the total energy calculations versus c/a, where A, B, B', C and D are special points whose corresponding values of c/a are 1.208, 1.26, 1.30, 1.40 and 1.63, respectively.

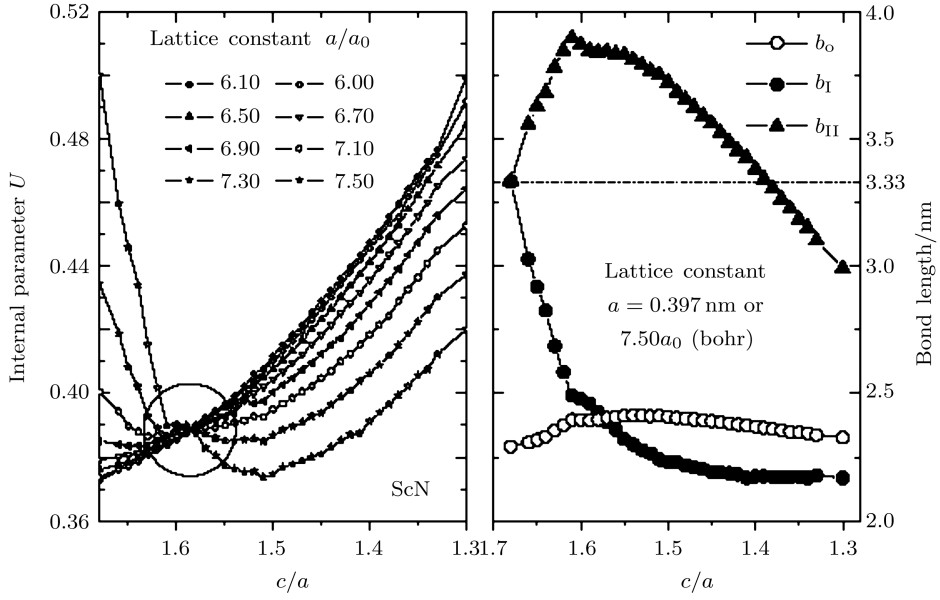


Fig.7. Curves for relaxed u and bond length (for $a = 0.397$ nm) as a function of c/a, where b_o is the length of the bond of h_o-ScN(noted as b_o), b_{II} is the length of the bond of WZ-ScN (noted as b_{II}) which is along the (001) direction, and the b_I is the length of the others bond of WZ-ScN (noted as b_I).

We can line out at two special points $B(c/a = 1.26)$ and $C(c/a = 1.40)$ in the left panel of Fig.6. The two lines partition the total range [1.68,1.208] into three subranges: $D \to C$, $C \to B$ and $B \to A$. Points $D(c/a = 1.63)$ and $A(c/a = 1.208)$ correspond to the ideal-WZ and ideal-h_o structures, respectively. We note that in the vicinity of ideal WZ (the range $D \to C$ in the right panel of Fig.6), the total energy, volume and u vary almost linearly with c/a. At the point where the crystal is compressed to the value of c/a reaching about 1.26 (i.e. at the point B in the right panel of Fig.6), u changes abruptly to a value of 1/2, where it then stays unchanged. This can be explained as follows. As we discussed, the material has a tendency to form more bonds because of the ionic nature of the bonding that is insensitive to direction.

And therefore the lower energy corresponds to a higher nearest-neighbouring coordination number. However, when c/a is close to the value for the ideal WZ structure and $u = 1/2$, h_o-ScN is formed, which would stretch the bond too far. The bond length will reach 0.341 nm, thus forming h_o-ScN at $c/a = 1.68$ (Fig.7).

As we reduce c/a, two bonds, instead of single wing, are formed (u suddenly changes to 1/2). In this step of transformation, the total binding energy (the opposite of cohesive energy) reduces monotonically from WZ-ScN to h_o-ScN : between them there exists a difference of 0.265 eV/(2 atoms) in binding energy, which is in good agreement with the earlier result (0.261 eV/(2 atoms)).[6] We may also note that the total energy and the volume change rapidly beyond $c/a \approx 1.4$ (at point C in the right panel of Fig.6), i.e. exactly when the curve for u versus c/a starts to deviate strongly from the initial linear variation and rapidly approach a constant value of 1/2. Also, this point more or less corresponds to the inflection point of the curve for volume versus c/a. The left panel in Fig.8 shows the curve for bond length versus c/a for each 'energy favourable' structure. It is noted that in the vicinity of ideal WZ (the range $D \to C$), the bond lengths of b_o (nearly in plane) and b_I (parallel to c) are almost unchanged.

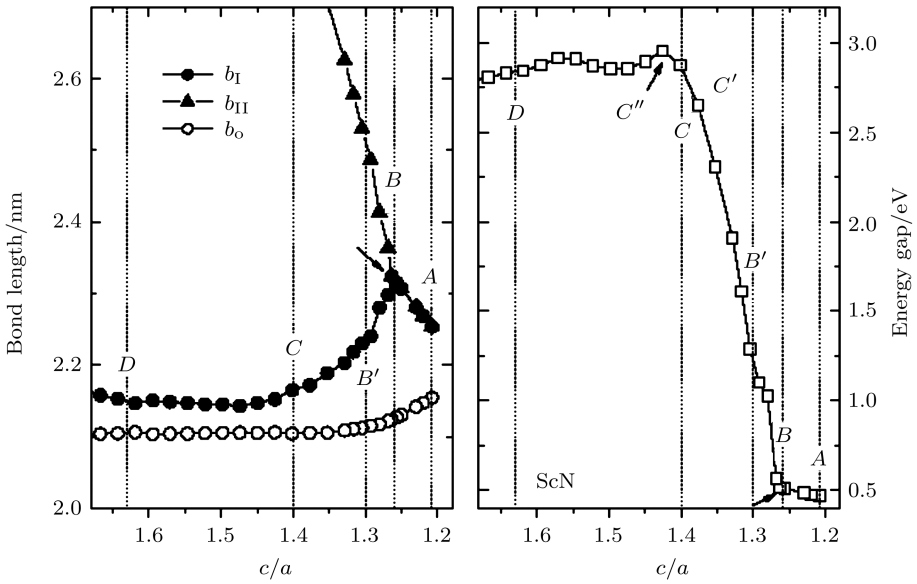


Fig.8. Band gap properties in the WZ-ScN→ h_o-ScN transition.

In the range $C \to B$, the length of b_I increases more rapidly than b_o and the b_I 's length equals the b_{II} 's length at point B. The characteristic of bond can be incarnated into the optical properties in the following section. The curve for bond length versus c/a for $a = 4$ a.u. is shown in the right panel of Fig.7, we can find that at a large value of c/a, the b_I 's length equals the b_{II} 's length and the structure becomes h_o. But the total energy is too high because the bond length is too large to form a bond.

4.2.2. Energy band properties

To further understand the nature of the transition, we examine the energy band properties of ScN along this transformation path. The band gap properties in the WZ-ScN → h_o-ScN transition is shown in Fig.8. Volume compression reduces the gap (see Table 3) because the hydrostatic deformation potential perhaps is positive in h_o-ScN, but increases the gap because the hydrostatic deformation is negative in WZ-ScN. The uniaxial c/a reduction on the other hand tends to reduce the gap because the splitting of the valence band increases. Under a large c/a compression, the Γ_1 singlet and Γ_6 doublet states are interchanged for their ordering at equilibrium ($\Gamma_6 > \Gamma_1$). The slope of the Γ_1 energy as a function of c/a is twice that of the Γ_6.[30] For the large distortion considered here, these effects are comparable in magnitude but with opposite sign. Also the c/a distortion changes the bands at other k points, lending to a different indirect gap location.

It is noted that in a range of $c/a > 1.40$ ($C \to D$), the value of band gap oscillates slightly around 2.80 eV, which accords with the characters of bond

length. In a range of $B \rightarrow C$, the band gap changes rapidly from about 0.5 eV to about 2.80 eV while c/a increases from 1.26 to 1.40. It is indicated that there is a large structure transformation in this range. For the structure changing from $B \rightarrow A$, there is a little increase in gap due to the positive hydrostatic deformation potential in the approximation of -$h_{\rm o}$-ScN.

The band structures of the intermediate structures which belong to the special values of c/a, i.e. $A(c/a = 1.20)$, $B'(c/a = 1.30)$, $C'(c/a = 1.39)$, $C(c/a = 1.40)$, $C"(c/a = 1.41)$ and $D(c/a = 1.63)$ (see Fig.8) are shown in Fig.9. First, we can see that the top valence-band width decreases when the structure changes from A to D. It is due to the increase of unit volume. For the intermediate structures of A, B' and C', the VBMs are all located at Γ and the CBMs are all located at K. For B' and A, the shapes of energy band are quite similar to each other, but for B' and C', the shapes are quite different from each other. Then we suggest that the structure of A or B' is different from that of C'. For the intermediate structures of C, $C"$ and D, the VBMs are all located at point M and the CBMs are located at K, Σ and Σ' (farther from M), respectively. So we suggest that perhaps there will be a structure with a direct band gap at point M for ScN in a region $C \rightarrow C"$. The shape of the labelled conductive band of $C"$, which is patternless from Γ point to K point, is different from that of C (or D). The bond length is hardly changed when the structural transformation of $C \rightarrow D$ takes place, so the bond angle will be a primary factor that causes the variation of energy band structures.

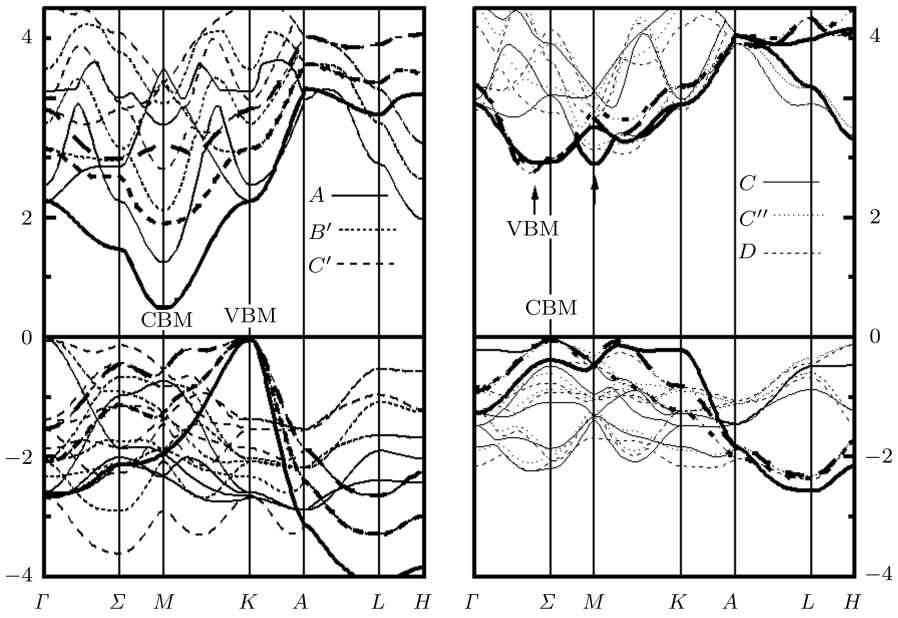


Fig.9. Energy band properties in the WZ-ScN $\rightarrow$ $h_{\rm o}$-ScN transition, where solid lines represent the bands of structure A in the left panel and C in the right panel, dot lines denote the bands of structure B' in the left panel and $C"$ in the right panel, dash lines refer to the bands of structure C' in the left panel and D in the right panel.

4.2.3. Difference charge densities

The difference charge densities are shown as contour plots superposed on a grey scale intensity image in the (110) plane cutting through atoms, and the intermediate structures of ScN, which are arrowed in Fig.9, are shown in Fig.10. It is noticed that for the structure of B point, which is nearly $h_{\rm o}$ structure, the bonding in the (001) plane (noted as $b_{\rm o}$ in Fig.6) is very ionic, but along the [001] direction it is little covalent (see Fig.10(a)). For the structure of B' point (see Fig.10(b)), the bond (denoted as $b_{\rm I}$ in Fig.6) between the N at the top-left (bottom-right) and the Sc at the middle-left (middle-right) starts to be destroyed, and another bond (denoted as $b_{\rm II}$ in Fig.6) becomes more ionic. The bond $b_{\rm I}$ is clearly destroyed for the structure of C point (see Fig.10(c)), and the angle between $b_{\rm I}$ and $b_{\rm o}$ is clearly larger than 90°. For the ideal wurtzite structure (D point, see Fig.10(d)), the bond b_I is almost similar to bond $b_{\rm o}$. So it is clear that

in the range $C \rightarrow B'$ the transition from a fourfold-coordinated structure to a fivefold-coordinated structure starts to appear, thereby forming a new bond that lowers the energy. And then this rapidly causes the volume to decrease faster, which further lowers the energy.

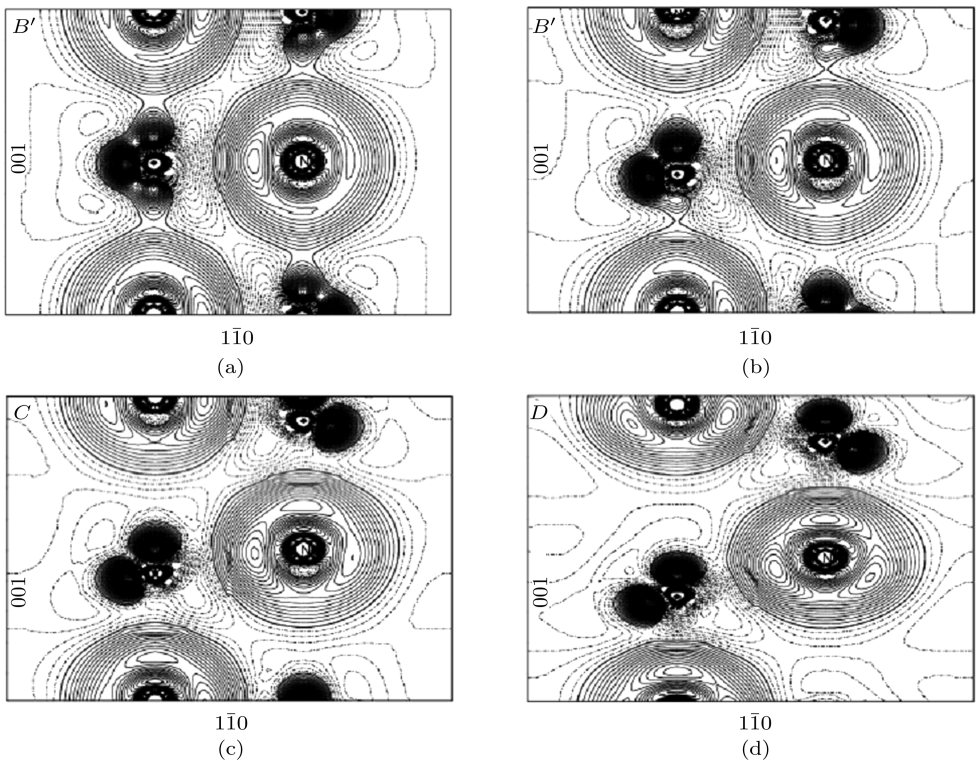
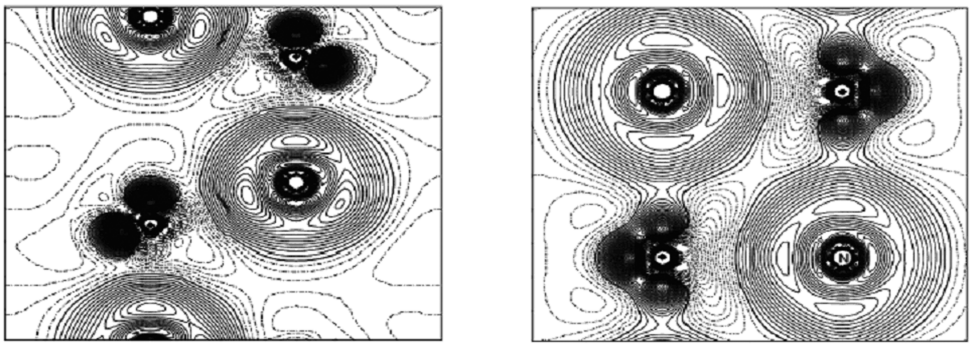
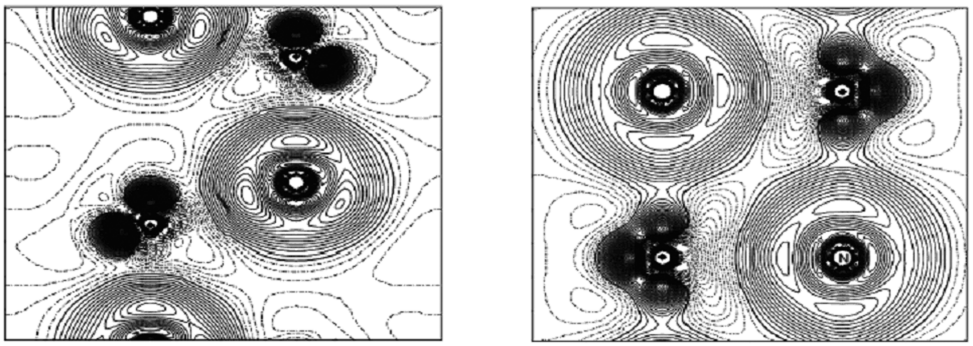


Fig.10. Plots of difference charge density in the (110) plane for the special structures which are shown in Fig.8. Here, panel (a) shows the structure of B point through the atoms, panel (b) describes the structure of B' point structure through the atoms, panel (c) illustrates the structure of C point structure the atoms, panel (d) displays the structure of D point structure through the atoms. The first (negative) contour line is at $-0.2\,\mathrm{e}\ a_\mathrm{o}^{-3}$ with a spacing of 0.01.

The curves for difference charge density for the WZ-ScN, h_o-ScN and RS-ScN structures are shown in Fig.11. It can be seen that for each structure there is an increase in electron density at the N atoms and a decrease in the interstitial region between the metal atoms. There is an decrease in electron density at Sc atoms for WZ-ScN and the [001] plane of h_o-ScN, but an increase for the (001) direction of h_o-ScN and RZ-ScN. So the bonding of WZ-ScN has an ionic-like character, the bonding of RS-ScN has a covalent-like character and the bonding of h_o-ScN are various in different directions. It is essential due to the bond length between N atoms and Sc atoms. When the bond length decreases, there will be a significant charge transfer to the more electronegative nitrogen atom.





(a) (b)

Fig.11. Plots of difference charge density of ScN, where panel (a) shows the WZ structure in the (110) plan through the atoms, panel (b) displays the h_o structure in the (110) plane through the atoms, panel (c) exhibits the h_o structure in the (001) plane through the atoms, panel (d) illustrates the RS structure in the (001) [or (110)] plane through the atoms. The first (negative) contour line is at –0.1 e a_o^{-3} with a spacing of 0.01.

The formation of the sixth bond results from the compression of h_o-ScN in the direction perpendicular to the crystal c axis. Hence it is easier to see in a plot of the difference charge density in the basal plane. Figure 11(a) shows the plots of difference charge density in the (001) plane through atoms of h_o-ScN, and Fig.11(c) displays the same plot of RS-ScN. We can see that an additional bond between Sc at the top-left corner and N at the bottom-left corner is clearly formed as we move from h_o-ScN to RS-ScN.

4.3. Summary of results about ScN

It is clear that the transition from the ideal WZ-ScN to RS-ScN is driven by the new bonds formation. Firstly, the energy decreasing monotonically in the compression along c/a indicates that the fourfold bonding is unstable for ScN. Secondly, a small activation energy in compressing b/a indicates a metastability of the fivefold coordinated h_o-ScN, which is followed by the rapid formation of the final sixth bond ending up in a preferred rocksalt structure. It accords with the result in Ref.[6], where the nearly five-times coordinated hexagonal structure is (meta) stable in ScN. Along the way, the equilibrium volume keeps decreasing, and it decreases more rapidly in the region where the new bonds start forming. The formation of new bonds is characterized by the increase of valence band width and the downward shift of the N 2s band. Overall, there is a tendency towards a more symmetric distribution of the bonds around each atom.

The band structures indicate an overall decrease in gap with compression. It is due to the valence-band splitting under uniaxial c/a compression, indicating the dominance of c/a distortions over volume compression effects. From the ideal WZ-ScN to h_o-ScN, the location of the indirect band gap is shifted due to the changes of the top-valence-band slop and the bottom-conduction-band slope. It is important to investigate the relation between c/a distortion and the slope of energy band in IBZ. And the band gap energy changes continuously from about 1 eV to about 4 eV, it will be used for the band-gap engineering.

5. Conclusion

In this paper, we have investigated the relative stabilities of rocksalt, h_o and wurtzite in ScN, and the transitions from wurtzite structure to h_o structure. The main conclusions for the semiconductor compound ScN are as follows. The wurtzite structure is unstable but there is a meta-stable structure closely related to it, which is denoted with h_o-ScN. The difference between them is an additional mirror plane or the fact that the basal plane layers are flat or that the wurtzite internal parameter u is equal to 1/2. It means that for this compound the fivefold coordination is preferred over a fourfold bonding. By examining the evolution of the minimum energy volume and u as a function of c/a, the sudden formation of an additional bond is evidential. The charge densities and band structures as a function of c/a are presented and they provide additional evidence of bond formation. Next, it is shown that an additional uniaxial compression in the basal plane along the $[1\bar{1}0]$ direction converts the structure into the stable rocksalt structure accompanied with forming one more bond. The bond formation is shown by charge densities. In the formation of new bonds, the system also undergoes

a faster reduction in volume because of the bond contraction. The bondings of WZ-ScN and RS-ScN have the ionic-like and the covalent-like characters, respectively. And the bondings of h_o-ScN are various in directions. Here we have presented the charge densities along this transformation path, which again evidences the formation of additional bonds. We have also discussed the band structures from the wurtzite phase to h_o phase. The changes in band structure are discussed by using the known deformation potentials and the influence of c/a distortions. It is found that the deformation potentials perhaps are positive for RZ-ScN and h_o-ScN, but they are negative for WZ-ScN. The location of the indirect gap changes from $M \to \Sigma$ to $\Gamma \to K$ while c/a becomes less than 1.4. This could be an indication of the transition. Also the band gap changes from about 1 eV to about 4 eV monotonously when c/a increases from about 1.26 to about 1.40. The transition model of ScN from wurtzite structure to h_o structure which we proposed will be proved by the further experiment, and the details of band structure, presented here, could be useful for this purpose.

References

[1] Gall D, Petrov I, Madsen L D, Sundgren J E and Geene J E 1998 *J. Vac. Sci. Technol.* A **16** 2411

[2] Gall D, Petrov I, Hellgren N, Hulman L, Sundgren J E and Geene J E 1998 *J. Appl. Phys.* **84** 6034

[3] Moustakas T D, Molna R J and Dismukes J P 1996 *Proc. Electrochem. Soc.* **96-11** 197

[4] Stampfl C, Mannstadt W, Asahi R and Freeman A 2001 *Phys. Rev.* B **63** 155106

[5] Lambrecht W R L 2000 *Phys. Rev.* B **62** 13538

[6] Farrer N and Bellaiche L 2002 *Phys. Rev.* B **66** 201203(R)

[7] Gall D, StÄaele M, JÄarrendahl K, Petrov I, Desjardins P, Haasch R T, Lee T Y and Greene J E 2001 *Phys. Rev.* B **63** 125119

[8] Wentzcovitch R M, Fahy S, Cohen M L and Louie S G 1988 *Phys. Rev.* B **38** 6191

[9] Takeuchi N 2002 *Phys. Rev.* B **65** 045204

[10] Limpijumnong S and Lambrecht Walter R L 2001 *Phys. Rev.* B **63** 104103

[11] Ranjan V, Bellaiche L and Walter E J 2003 *Phys. Rev. Lett.* **90** 257602

[12] Ranjan V, Bin-Omran S, Bellaiche L and Ahmad Alsaad 2005 *Phys. Rev.* B **71** 195302

[13] Ranjan V, Bin-Omran S, Sichuga D, Nichols R S and Bellaiche L 2005 *Phys. Rev.* B **72** 085315

[14] Hohenberg P and Kohn W 1964 *Phys. Rev.* B **136** 864
Kohn W and Sham L J 1965 *Phys. Rev.* A **140** 1133

[15] Singh D J 1994 *Planewaves, Pseudopotentials and the LAPW Method.* (Boston (MA): Kluwer Academic)

[16] Blaha P, Schwarz K and Luitz J 1999 *WIEN97, A Full Potential Linearized Augmented Plane Wave Package for Calculating Crystal Properties. Karlheinz Schwarz, Techn.* (Austria: Universitat Wien)

[17] Perdew J P, Burke K and Ernzerhof M 1996 *Phys. Rev. Lett.* **77** 3865

[18] Table of Interatomic Distances and Configuration in Molecules and Ions, Supplement 1956-1959 edited by Sutton L E, Special Publication No. 18 (London: Chemical Society 1965)

[19] Lengauer W 1988 *J. Solid State Chem.* **76** 412

[20] Gubanov V A, Lu Z W, Klein B M and Fong C Y 1996 *Phys. Rev.* B **53** 4377

[21] Park K T, Terakura K and Hamada N 1984 *J. Phys.* C **20** 1241

[22] Schilfgaarde M van, Sher A and Chen A B 1997 *J. Cryst. Growth* **178** 8

[23] Wyckoff R W G *Crystal Structures* 1963 2nd ed. (New York: Wiley) Vol.**1** p86

[24] Villars P and Calvert L D 1985 *Pearson's Handbook of Crystallographic Data for Intermetallic Phases* (Metals Park, OH: American Society for Metals)

[25] Perdew J P and Levy M 1983 *Phys. Rev. Lett.* **51** 1884

[26] Sham L J and SchlÄuter M 1983 *Phys. Rev. Lett.* **51** 1888

[27] Godby R W, SchlÄuter M and Sham L J 1988 *Phys. Rev.* B **37** 159

[28] Little M E and Kordesch M E 2001 *Appl. Phys. Lett.* **78** 2891

[29] Constantin C, Al-Brithen H, Haider M B, Ingram D and Smith A R 2004 *Phys. Rev.* B **70** 193309

[30] Kim K, Lambrecht W R L, Segall B and Schilfgaarde M van 1997 *Phys. Rev.* B **56** 7363